

Equivalent Circuit Modeling and Experimental Analysis of Low Frequency Metamaterial for Efficient Wireless Power Transfer

Webster O. Adepoju, Indranil Bhattacharya, Ebrahim E. Nasr, Olatunji Abiodun, Trapa Banik
Electrical and Computer Engineering Department

OBJECTIVES

- ✓ to design a compact, low frequency metamaterial (MM)-based wireless power transfer (WPT) system
- ✓ to derive an equivalent circuit representation and mathematical model of a MM-based WPT system.
- ✓ to determine the analytical solution of the transmission scattering parameter and power transfer efficiency of an MM-based WPT system.

INTRODUCTION

MM-based Wireless Power Transfer (WPT) has demonstrated tremendous capability as an efficient power transmission mechanism in consumer electronics, body implants and wireless charging of Electric Vehicles [1].



Figure 1: Common Application of WPT

- Limitations:**
- high power dissipation, high switching loss and component stress
 - radio and microwave operating frequency resulting in reduced efficiency
 - increased risk of exposure to high frequency EM radiation

- Proposed Solution:**
- design a kilohertz frequency compact metamaterial to minimize the switching loss, reduce component stress while enhancing transmit power and power transfer efficiency (PTE)
 - Use a physics based approach to mitigate the effect of reactive parameters on transfer power

WPT Performance Enhancement with Meta-material (MM)
Generally, MM(s) are typically characterized by negative refractive index, a culmination of negative effective permeability (μ_{eff}) and effective permittivity (ϵ_{eff}) which are holistically harnessed for coupling, amplification and focusing of near magnetic flux lines in a directional. A decoupling of μ_{eff} and ϵ_{eff} in deep sub-wavelength region implies that a negative value of either μ_{eff} or ϵ_{eff} is sufficient for MM characterization. This concept is referred to as evanescent wave amplification.

Main Contribution
Specifically, the main contribution of this work is the design of an equivalent circuit model to emulate the behavior of a MM-based WPT system. While interference and effective medium theories have been exploited to explain the physics mechanism of MM-based WPT systems, some of the reactive parameters and the basic physical interpretation have not been clearly expounded. The proposed approach focuses on the effect of the system parameters and transfer coils on the system transfer characteristics and its effectiveness in analyzing complex circuit.

METHODOLOGY

Fig. 2 exemplifies the steps involved in research implementation. Finite Element Analysis (FEA) and electromagnetic (EM) simulation design is conducted in HFSS.



Figure 2: Procedural Approach to Research Implementation

- MM characteristics:**
- High μ Ferrite, negative refractive index
- Test bench requirement:**
- Type: Litz wire, network analyzer, probe

REFERENCES

- [1] Webster Adepoju, Indranil Bhattacharya, Mary Sanyaolu, Bima Muhammad, Trapa Banik, Ebrahim N. Eshfahani, and Olatunji Abiodun. Critical review of recent advancement in metamaterial design for wireless power transfer. *IEEE Access*, pages 1–1, 2022.

SYSTEM MODELING

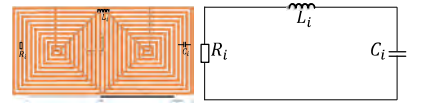


Figure 3: proposed unit MM cell unit cell modeled as RLC parameter

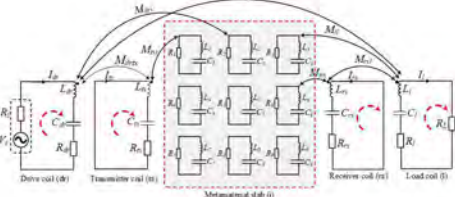


Figure 4: Equivalent circuit schematic of the proposed four coil structure. The MM slab is derived from a 3x3 periodic array of the unit cell

Model Description:
In the presented equivalent circuit model, the proposed unit MM cell is modeled into coupling coils. Each coupling coil (unit cell) is modeled as a resistance, R_i ($i = 1, 2, 3, \dots, 9$), inductor, L_i ($i = 1, 2, 3, \dots, 9$), and capacitor, C_i ($i = 1, 2, 3, \dots, 9$). RLC resonant parameters as exhibited in Fig. 3. Subscript i represents each unit cell in the MM-slab.
As shown in (1), the resistive component consists of the ohmic loss (R_o) and dielectric loss (R_d) due to the copper coil.
Similarly, the capacitive component is modeled as the sum of the stray capacitance (C_s) and compensation capacitor C_{comp} .
The MM-slab can be considered as a achieving repeater coils or booster network for achieving evanescent wave amplification of near magnetic field for increased power transfer.
The current flow through each unit cell of the MM-slab can be assumed identical and in phase while the overall system can be represented as a lump circuit model.
Given that the weak magnetic coupling between two non-adjacent coils, the corresponding mutual inductance is assumed to be zero as depicted in (3)

Mathematical Analysis

$$R_i = R_o + R_d \quad C_i = C_s + C_{comp}$$

$$Z_{Tx} = R_{Tx} + j[\omega L_{Tx} - (\omega C_{Tx})^{-1}]$$

$$Z_{Dr} = R_{Dr} + j[\omega L_{Dr} - (\omega C_{Dr})^{-1}]$$

$$Z_L = R_L + R_d + j[\omega L_L - (\omega C_L)^{-1}]$$

$$Z_i = R_i + j[\omega L_i - (\omega C_i)^{-1}]$$

$$M_{dr1} = M_{Lr1} = M_{Lr2} = M_{Lr3} = 0$$

$$\% \eta = |S_{21}|^2 \times 100\%$$

FINITE ELEMENT SIMULATION

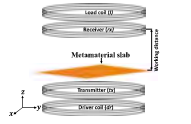


Figure 5: Schematics HFSS simulation of the proposed MM-based WPT system. The MM-slab is situated between the resonant coils. The dimension of the MM slab is $128 \times 96 \text{ mm}^2$

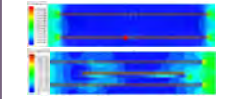


Figure 6: Magnetic field distribution in a four coil WPT structure (upper) without MM-slab (lower) with MM-slab

Table 1: Parameter Specification

Parameter	Symbol	Unit	Value
Inductance	L_{Tx}	nH	0.7
	L_D	nH	1.09
	L_{Dr}	nH	4
Capacitance	C_{Tx}	pF	40
	C_D	pF	100
Resistance	R_o	Ω	50
	R_r	Ω	0.05
	R_i	Ω	40

EM simulation Procedure:
Fig. depicts a 3-D electromagnetic simulation of the proposed equivalent circuit. In addition, the simulation parameters in Table 1 are consistent with the IEEE standard criterion of 5% for ripple minimization. The accuracy of the transmission coefficient (S_{21}) and power transfer efficiency (η) are investigated based on model analysis and Electromagnetic (EM) simulation.

For the entire simulation, the magnetic air-gap between the transmitting coil and MM-slab is varied from 100mm to 250mm. As seen in Fig. 6, the magnetic field distribution is more concentrated and about $\times 10$ larger with the insertion of MM-slab in comparison to conventional WPT systems.

TRANSMISSION COEFFICIENT, S_{21}

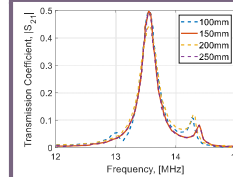


Figure 7: Plot of S_{21} as a function of frequency for varying transfer distance
The maximum value of S_{21} is observed to correspond to a resonant frequency, $f_o \approx 13.6 \text{ MHz}$.

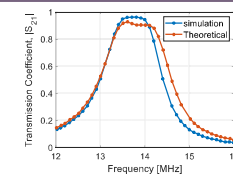


Figure 8: Comparison plot showing the calculated and simulated S_{21} against frequency
Obtrusively, the value of S_{21} is closely related to the loading position of the MM-slab.

EFFICIENCY, η

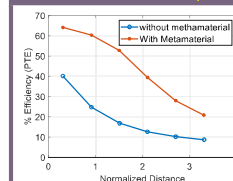


Figure 9: Comparison of efficiency (PTE) against normalized distance with and without MM

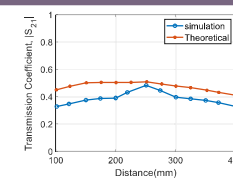


Figure 10: Comparison waveforms of calculated and simulated S_{21} versus transfer distance.

EFFECTIVE PERMEABILITY, μ_{eff}

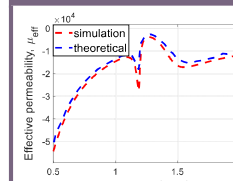


Figure 11: Comparison of calculated and simulated effective permeability versus frequency

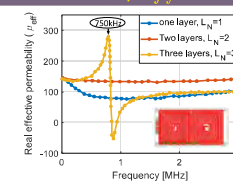


Figure 12: Waveform showing the influence of optimization of design parameters on MM resonant frequency and μ_{eff}

EXPERIMENTAL TEST-BED

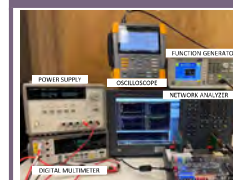


Figure 13: Prototype Test-bed of the proposed MM-based WPT system



Figure 14: Phase and Magnitude plot of reflection, S_{11} , showing 793kHz resonant frequency

PROTOTYPE RESULT AND ANALYSIS

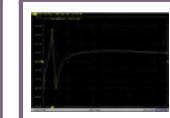


Figure 15: Prototype Test-bed of the proposed MM-based WPT system

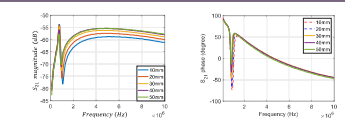


Figure 16: S_{21} magnitude versus frequency for varying T_x to MM-slab distance



Figure 18: Prototype Test-bed of the proposed MM-based WPT system

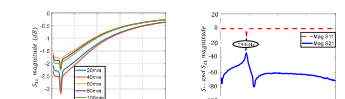


Figure 19: S_{11} magnitude versus frequency under varying T_x to MM-slab distance



Figure 21: Experimental measurement of PTE, output power and output voltage

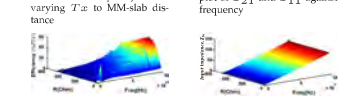


Figure 22: 3D plot of power transfer efficiency under varying load resistance and frequency

Fig. 15 - Fig. 23 clearly demonstrate the frequency reduction effect (793kHz) of the MM-slab on the measured parameters

DISCUSSION OF RESULTS

- the proposed novel low frequency MM-based WPT system demonstrates higher mutual coupling, transfer power, and power transfer efficiency compared to existing MM design
- inherently high magneto-inductive wave increases the magnetic field density due to the transmitting coil and enhances near field coupling.
- The MM consistently demonstrate 793kHz resonant frequency under varying operating distance
- close matching of the theoretical and calculated S_{21} and S_{11} magnitude validates the accuracy of the theoretical model

CONCLUSION

- Significantly low resonant frequency, enhanced coupling and PTE have been realized with the proposed MM compared to existing MM structures
- Accurate equivalent circuit model/analysis had been proposed to emulate the physics behavior of MM

FUTURE RESEARCH

- resonant frequency mitigation to 85kHz, making it adaptable for high power application.
- investigate the optimal positioning of the MM slab for enhanced coupling and power loss mitigation

ACKNOWLEDGMENT

Special thanks goes to Department of Electrical Engineering and Carnegie Foundation Fellowship, TN